Quassinoids from the Roots of *Eurycoma longifolia* and Their Anti-Proliferation Activities

Wei-Qun Yang [1,2,3,†], Wei Tang [2,3,†], Xiao-Jun Huang [2,3], Jian-Guo Song [2,3], Yue-Yue Li [2,3], Yu Xiong [2,3], Chun-Lin Fan [2,3], Zhen-Long Wu [2,3,*], Ying Wang [2,3,*] and Wen-Cai Ye [2,3]

1 School of Pharmaceutical Sciences, Guangzhou University of Chinese Medicine, Guangzhou 510006, China; yangwq_zzy@gzucm.edu.cn

2 Center for Bioactive Natural Molecules and Innovative Drugs Research, College of Pharmacy, Jinan University, Guangzhou 510632, China; tangv163@163.com (W.T.); zhyxiaohuang@163.com (X.-J.H.); songjianguof403@126.com (J.-G.S.); liyueyue7991@163.com (Y.-Y.L.); xyu0218@163.com (Y.X.); jnuchunlin@163.com (C.-L.F.); chywc@aliyun.com (W.-C.Y.)

3 Guangdong Province Key Laboratory of Pharmacodynamic Constituents of TCM and New Drugs Research, College of Pharmacy, Jinan University, Guangzhou 510632, China

* Correspondence: zhenlongwu@jnu.edu.cn (Z.-L.W.); wangying_cpu@163.com (Y.W.); Tel.: +86-20-8522-1559 (Y.W.)

† These authors contributed equally to this work.

Abstract: A phytochemical investigation on the roots of medicinal plant *Eurycoma longifolia* resulted in the isolation of 10 new highly oxygenated C_{20} quassinoids longifolactones G-P (**1–10**), along with four known ones (**11–14**). Their chemical structures and absolute configurations were unambiguously elucidated on the basis of comprehensive spectroscopic analysis and X-ray crystallographic data. Notably, compound **1** is a rare pentacyclic C_{20} quassinoid featuring a densely functionalized 2,5-dioxatricyclo[5.2.2.0^{4,8}]undecane core. Compound **4** represents the first example of quassinoids containing a 14,15-epoxy functionality, and **7** features an unusual α-oriented hydroxyl group at C-14. All isolated compounds were evaluated for their anti-proliferation activities on human leukemia cells. Among the isolates, compounds **5**, **12**, **13**, and **14** potently inhibited the in vitro proliferation of K562 and HL-60 cells with IC_{50} values ranging from 2.90 to 8.20 μM.

Keywords: *Eurycoma longifolia*; Simaroubaceae; quassinoids; natural products; anti-proliferation activities

1. Introduction

Quassinoids are a class of highly oxygenated degraded triterpenoids mainly distributed in plant family Simaroubaceae [1]. Based on the number of carbon atoms involving the construction of their basic scaffolds, quassinoids are commonly categorized into six distinct groups: C_{26}, C_{25}, C_{22}, C_{20}, C_{19}, and C_{18} types [2]. Quassinoids have been reported to display a wide range of biological activities, including antitumor, antimalarial, anti-inflammatory, antiviral, neuroprotective, and antifeedant activities [2,3]. Especially since the discovery of bruceantin, a C_{20} quassinoid isolated from *Brucea antidysenteria* (Simaroubaceae) in the early 1970s that showed remarkable antileukemic activity, the antitumor activities of quassinoids have attracted extensive attention from both chemical and biological communities [4–7].

Eurycoma longifolia Jack (Simaroubaceae), commonly known as "Tongkat Ali", is a flowering shrub plant that widely distributed in Southeast Asia [8]. The roots of *E. longifolia* were traditionally used by local people for the treatment of malaria, dysentery, glandular swelling, persistent fever, aches, and sexual insufficiency [8]. Besides, the antitumor activities of the crude extract of *E. longifolia* roots were reported in 2005 [9]. Previous phytochemical investigations on the roots of *E. longifolia* have afforded a wide variety of chemical components, including quassinoids, canthin-6-one alkaloids, β-carboline alkaloids,

tirucallane-type triterpenes, squalene derivatives, and biphenyl neolignans [10]. Among them, quassinoids are the most characteristic chemical constituents of this plant [11–13].

Previously, our group had reported the isolation and characterization of six novelquassinoids (longifolactones A-F) with unprecedented C_{26} or C_{20} scaffolds from the petroleum ether-soluble fraction of the ethanol extract of *E. longifolia* roots [14]. Among them, longifolactone F is the first example of quassinoids containing an unprecedented densely functionalized 2,5-dioxatricyclo [5.2.2.0^{4,8}]undecane ring system. In our continuing studies on searching structurally unique and biologically interesting metabolites from medicinal plants, the ethyl acetate-soluble fraction of the title plant was further investigated. As a result, longifolactones G-P (**1–10**), 10 new C_{20} quassinoids, together with four known ones were isolated. Their structures and absolute configurations were unambiguously established by extensive spectroscopic data analysis and single-crystal X-ray diffraction experiment. Notably, compound **1** is the second member of the rare class of quassinoids featuring densely functionalized 2,5-dioxatricyclo[5.2.2.0^{4,8}]undecane core. Besides, compound **4** represents the first example of quassinoids containing a 14,15-epoxy functionality, and compound **7** features an unusual 14α-OH substituent that makes **7** the second member of this rare class of quassinoids so far. Herein, we reported the isolation and structure elucidation of these new quassinoids. In addition, the in vitro anti-proliferation activities of all isolates on two human leukemia cell lines (K562 and HL-60 cells) were also described.

2. Results and Discussions

2.1. Quassinoids Isolated from E. longifolia

The air-dried and powdered roots of *E. longifolia* (10 kg) were extracted with 95% ethanol under room temperature for five times. The ethanol extract (270 g) was suspended in water and partitioned successively with petroleum ether, ethyl acetate, and *n*-butanol. The ethyl acetate-soluble fraction was investigated in present study. By performing a series of charomatographic procedures on the aforementioned fraction, 10 new C_{20} quassinoids (longifolactones G-P, **1-10**), along with four known C_{20} quassinoids, chaparrolide (**11**) [15], 15β-hydroxyklaineanone (**12**) [16], 14,15β-dihydroxyklaineanone (**13**) [17], and eurycomanone (**14**) [18], were isolated (Figure 1).

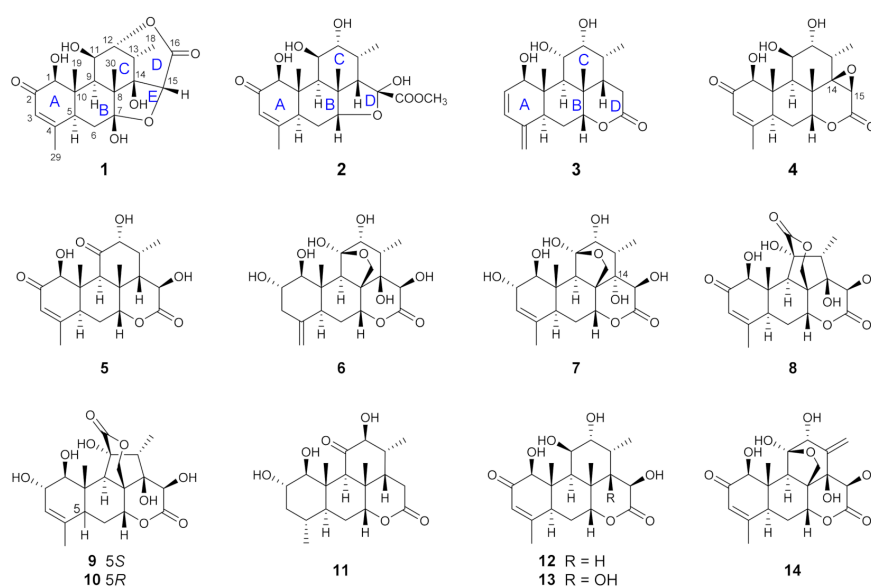**Figure 1.** Chemical structures of quassinoids isolated from the roots of *E. longifolia*.

2.2. Structure Elucidation of the New Quassinoids

Compound **1** was obtained as colorless needles. Its molecular formula was determined as $C_{20}H_{26}O_8$ by the HR-ESI-MS ion peak at *m/z* 395.1696 [M + H]$^+$ (calcd for $C_{20}H_{27}O_8$, 395.1700) and ^{13}C NMR data. The UV spectrum of **1** displayed absorption maxima at

241 nm. Its IR spectrum revealed the characteristic absorptions for hydroxyl (3455 cm^{-1}) and carbonyl (1730 and 1667 cm^{-1}) functional groups. In the ^{1}H and ^{13}C NMR spectra of **1**, signals corresponding to two hydroxyl groups [δ_H 7.05 (1H, s) and 6.89 (1H, d, J = 5.7 Hz)], a ketone carbonyl (δ_C 199.7), a ester carbonyl (δ_C 171.5), a trisubstituted double bond [δ_H 6.07 (1H, br s); δ_C 163.3 and 125.6], a hemiketal carbon (δ_C 111.0), an oxygenated quaternary carbon (δ_C 82.9), four oxygenated methines [δ_H 5.45 (1H, m), 5.13 (1H, s), 4.72 (1H, dd, J = 4.6, 1.8 Hz), and 4.00 (1H, s); δ_C 85.5, 83.5, 82.7, and 69.5], three methines, a methylene, two quaternary carbons, and four methyl groups [δ_H 1.96 (3H, s), 1.70 (3H, s), 1.39 (3H, s), and 1.34 (3H, d, J = 7.2 Hz); δ_C 21.6, 13.0, 12.9, and 12.8] were observed, indicative of a C$_{20}$ quassinoid skeleton for **1**. With the aid of 2D NMR spectroscopic data, all proton and carbon resonances of **1** were assigned (Tables S1 and S2).

The above NMR spectroscopic data of **1** were closely similar to those of longifolactone F [14], suggesting the structural similarity of these two compounds. Different from longifolactone F, the NMR signals corresponding to a methylene group (CH$_2$-3) and a methine group (CH-4) were replaced by resonances of a double bond [δ_H 6.07 (1H, br s); δ_C 163.3 and 125.6] in **1**. In the HMBC spectrum, key correlations between H$_3$-29 and C-3, H-5 and C-3, H$_2$-6 and C-4 were observed, suggesting the presence of an α,β-unsaturated ketone motif in ring A of **1**, which was also confirmed by the characteristic chemical shift values of C-2-C-4 (δ_C 199.7, 125.6, and 163.3). After a comprehensive interpretation of its ^{1}H–^{1}H COSY and HMBC spectra, the gross structure of **1** was established as a C$_{20}$ quassinoid with a rare 2,5-dioxatricyclo[5.2.2.0^{4,8}]undecane core (Figure 2).
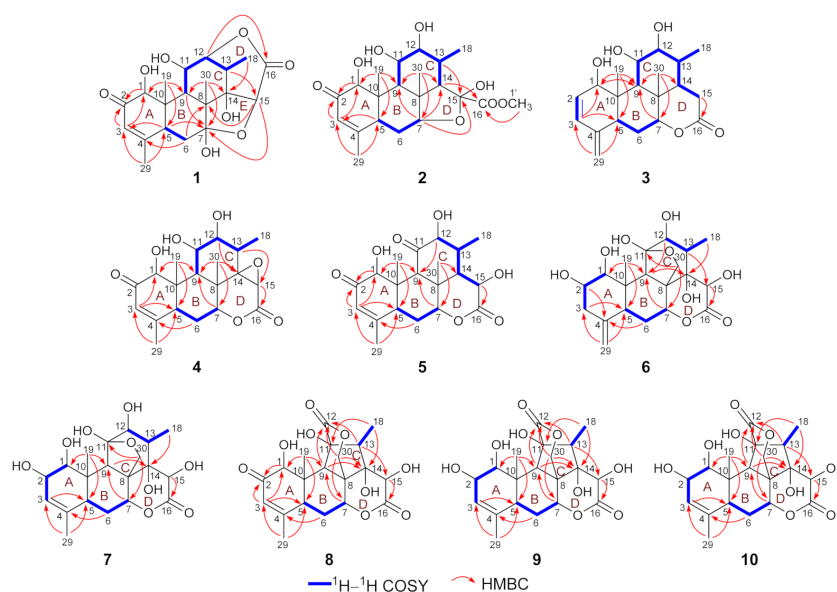

Figure 2. Key ^{1}H–^{1}H COSY and HMBC correlations of compounds **1–10**.

In the NOESY spectrum of **1**, key NOE correlations between H-1 and H-5/H-11, H-5 and H-9 were observed, indicating that these protons had the same orientation. Meanwhile, the NOE correlations between OH-14 and H-15/H$_3$-30, H-13 and H$_3$-30, H$_3$-19 and H$_3$-30 were observed, suggesting that these protons were located on the same face of the molecule (Figure 3). Finally, suitable crystals of **1** were acquired. The following X-ray diffraction analysis with Cu Kα radiation resulted in an excellent Flack parameter of 0.06 (4), which not only allowed the verification of the planar structure of **1** but also led to the establishment of its absolute configuration as 1*S*,5*S*,7*R*,8*R*,9*R*,10*S*,11*R*,12*R*,13*S*,14*R*,15*R* (Figure 4).
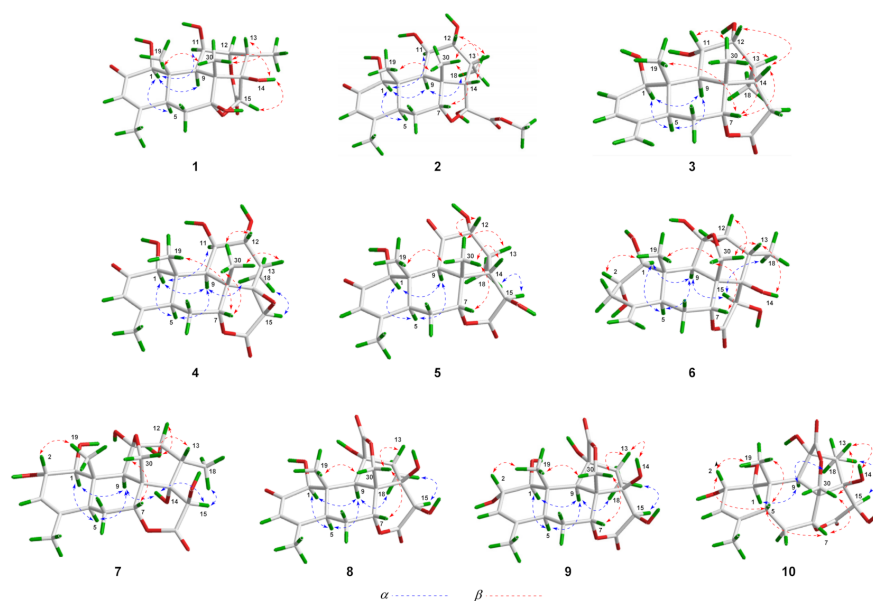
Figure 3. Key NOESY correlations of compounds **1–10**.
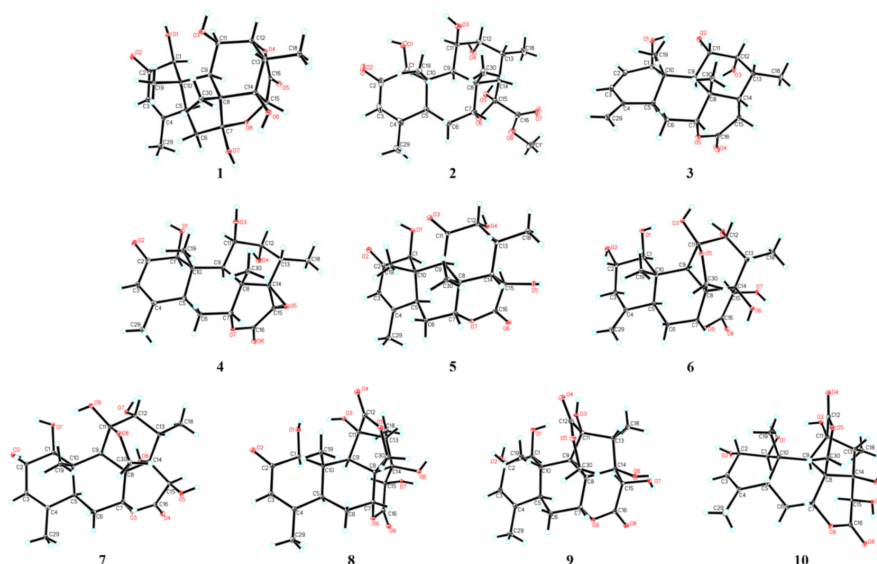

Figure 4. X-ray ORTEP drawings of compounds **1–10**.

The molecular formula of **2** was deduced as $C_{21}H_{30}O_8$ on the basis of its HR-ESI-MS data (*m/z* 433.1832 [M + Na]+; calcd for $C_{21}H_{30}O_8Na$, 433.1833), and the ¹³C NMR data analysis. The ¹H and ¹³C NMR spectroscopic data of **2** (Tables S1 and S2) highly resembled those of 6-dehydroxylongilactone [19], except for the presence of additional signals due to a hemiketal carbon (δ_C 102.5) and an oxygenated methyl group [δ_H 3.83 (3H, s); δ_C 52.7] in **2**. Subsequently, detailed analysis of its ¹H–¹H COSY and HMBC spectra allowed the establishment of a 6/6/6/5 ring system for **2** that was identical to 6-dehydroxylongilactone. Besides, the HMBC correlation between 1′-OCH₃ and C-16 indicated the presence of an extra methoxycarbonyl group in **2**. Based on the molecular formula information, as well as the obvious down-field shift of C-15 (δ_C 102.5), the remaining methoxycarbonyl and hydroxyl groups were both assigned to attach to C-15, which was also confirmed by the HMBC correlation between H-14 and C-16 (Figure 2). Thus, the planar structure of **2** was established. Finally, the structure of **2** was fully resolved by an X-ray diffraction experiment.

With an excellent Flack parameter of 0.09 (8), the absolute configuration of **2** was assigned as 1*S*,5*S*,7*R*,8*R*,9*R*,10*S*,11*R*,12*R*,13*R*,14*S*,15*S* (Figure 4).

The molecular formula of **3** was determined to be $C_{20}H_{28}O_5$ on the basis of its sodiated molecular ion peak at *m/z* 371.1831 [M + Na]$^+$ (calcd for $C_{20}H_{28}O_5Na$, 371.1829) and ^{13}C NMR data. The ^1H and ^{13}C NMR spectral data of **3** were similar to those of the co-isolated known compound chaparrolide (**11**), which indicated that **3** was also a C_{20} quassinoid. Compared with those of **11**, the ^1H and ^{13}C NMR spectra of **3** showed additional signals for a *cis*-disubstituted double bond [δ_H 6.31 (1H, d, *J* = 9.6 Hz) and 5.76 (1H, d, *J* = 9.6 Hz); δ_C 132.7 and 130.2] and an *exo*-olefin group [δ_H 5.00 (1H, s) and 4.84 (1H, s); δ_C 145.8 and 111.3], while the signals corresponding to a ketone carbonyl, a methylene group, a methine group, and a methyl group were absent. In the ^1H–^1H COSY spectrum of **3**, the correlation between H-11 and H-12 indicated that the C-11 in **3** was an oxygenated-substituted methine instead of the ketone carbonyl in **11** (Figure 2). Moreover, the observed HMBC cross-peaks between H$_2$-29 and C-3/C-5, H-3 and C-5, H-3 and C-1 indicated the presence of two conjugated double bonds in ring A of **3** (Figure 2). Similarly, an X-ray diffraction experiment using Cu Kα radiation was performed, which led to the full assignment of planar structure and absolute configuration for **3** (1*R*,5*S*,7*R*,8*S*,9*R*,10*S*,11*S*,12*R*,13*R*,14*S*, Figure 4).

The molecular formula of **4** was assigned as $C_{20}H_{26}O_7$ based on its HR-ESI-MS data (*m/z* 401.1574 [M + Na]$^+$; calcd for $C_{20}H_{26}O_7Na$, 401.1571) and ^{13}C NMR spectroscopic data, 18 mass units less than the co-isolated known C_{20} quassinoid, 14,15β-dihydroxyklaineanone (**13**). The NMR spectra of **4** showed characteristic signals similar to those of **13**, except for the presence of one oxygen-bearing methine [δ_H 3.36 (1H, s); δ_C 52.9] and one oxygenated bearing quaternary carbon (δ_C 67.9). Considering the molecular formula information, the two hydroxyl groups at C-14 and C-15 in **13** were replaced by an epoxide ring in **4**. Furthermore, the NOE correlation between H-15 and H$_3$-18 in the NOESY spectrum suggested that the epoxide ring had the β-orientation (Figure 3). Similar to **1–3**, the structure with absolute configuration (1*S*,5*S*,7*R*,8*S*,9*R*,10*S*,11*R*,12*R*,13*S*,14*R*,15*R*) of **4** was definitively assigned by an X-ray diffraction experiment (Figure 4).

The molecular formula of **5** was determined as $C_{20}H_{26}O_7$ by the HR-ESI-MS ion peak at *m/z* 401.1574 [M + Na]$^+$ (calcd for $C_{20}H_{26}O_7Na$, 401.1571) and ^{13}C NMR data. The ^1H and ^{13}C NMR spectral data of **5** (Tables S1 and S2) were very similar to those of 11-dehydroklaineanone [20]. The main differences were that the signals corresponding to a methylene group [δ_H 3.69 (1H, dd, *J* = 19.4, 12.7 Hz) and 2.70 (1H, dd, *J* = 19.4, 6.6 Hz); δ_C 29.1] in the known compound were replaced by the signals due to an oxygenated methine [δ_H 5.42 (1H, d, *J* = 10.1 Hz); δ_C 67.3] in **5**, suggesting the presence of an additional hydroxyl group at C-15 in **5**. This assumption was further confirmed by the HMBC cross-peak between H-15 and C-16 (Figure 2). Subsequently, the planar structure and absolute configuration (1*S*,5*S*,7*R*,8*S*,9*R*,10*S*,12*R*,13*R*,14*S*,15*R*) of **5** were completely deduced by a single-crystal X-ray diffraction experiment (Figure 4).

The HR-ESI-MS of **6** displayed a sodiated molecular ion peak at *m/z* 435.1626 [M + Na]$^+$, corresponding to a molecular formula of $C_{20}H_{28}O_9$. Comparison of the ^1H and ^{13}C NMR spectral data of **6** (Tables S1 and S3) with those of $\Delta^{4,5}$,14-hydroxyglaucarubol [21] revealed that they were closely similar, except for signals for the *endo*-olefin (δ_C 130.1 and 127.5) and a methyl [δ_H 1.75 (3H, s); δ_C 20.2] in $\Delta^{4,5}$,14-hydroxyglaucarubol were replaced by signals of an *exo*-olefin [δ_H 4.98 (1H, s) and 4.74 (1H, s); δ_C 147.4 and 110.1] and a methine [δ_H 2.74 (1H, overlapped); δ_C 42.5] in **6**. In the HMBC spectrum, correlations between H$_2$-29 and C-3/C-5 indicated that the *exo*-olefin was located at C-4 (29) (Figure 2). Thus, the planar structure of **6** was established. Similarly, the relative stereostructure and absolute configuration (1*S*,2*S*,5*S*,7*R*,8*R*,9*R*,10*S*,11*R*,12*R*,13*S*,14*R*,15*R*) of **6** were established by a single-crystal X-ray diffraction experiment (Figure 4).

The molecular formula of **7** was deduced as $C_{20}H_{28}O_9$ by its HR-ESI-MS data (*m/z* 435.1621 [M + Na]$^+$; calcd for $C_{20}H_{28}O_9Na$, 435.1626) and ^{13}C NMR data. The NMR spectroscopic features of **7** were similar to those of 14-*epi*-13,21-dihydroeurycomanone [22], except for the presence of signals assigned to an oxygenated methine [δ_H 4.63 (1H, br s); δ_C 72.3]

in 7, while the signal corresponding to a ketone carbonyl carbon was absent. The above data suggested that **7** was the C-2 hydroxylated derivative of 14-*epi*-13,21-dihydroeurycomanone. This assumption was confirmed by the spin system deduced from H-1 to H-3 in the ^{1}H–^{1}H COSY spectrum of **7** (Figure 2). Furthermore, the NOE correlation between H-2 and H$_3$-19 in the NOESY spectrum suggested that the H-2 and H$_3$-19 had the same orientation (Figure 3). Finally, with a Flack parameter of −0.12 (9), the absolute structure of **7** (1*S*,2*S*,5*S*,7*R*,8*R*,9*R*,10*S*,11*R*,12*R*,13*S*,14*S*,15*R*) was unambiguously established (Figure 4).

The HR-ESI-MS of compound **8** displayed a sodiated molecular ion peak at *m/z* 431.1311 [M + Na]$^+$ (calcd for C$_{20}$H$_{24}$O$_9$Na, 431.1313), allowing the determination of a molecular formula of C$_{20}$H$_{24}$O$_9$ that was identical to the known C$_{20}$ quassinoid 13-*epi*-eurycomadilactone [21]. The ^{1}H and ^{13}C NMR spectral data of **8** (Tables S1 and S3) closely resembled those of 13-*epi*-eurycomadilactone, combined with its molecular formula information, suggesting that **8** was a stereoisomer of the known compound. Further analysis of the 2D NMR data of **8** confirmed that 8 had the same planar structure as 13-*epi*-eurycomadilactone. Different from 13-*epi*-eurycomadilactone, the NOESY spectrum of **8** showed the correlation between H-13 and H$_2$-30, indicating the α-orientation for the H$_3$-18 in **8** (Figure 3). The structure with absolute configuration (1*S*,5*S*,7*R*,8*R*,9*R*,10*S*,11*S*,13*R*,14*R*,15*R*) of **8** was finally determined on the basis of an X-ray crystallography study by using the anomalous dispersion of Cu Kα radiation (Figure 4).

Compound **9** was assigned to possess a molecular formula of C$_{20}$H$_{26}$O$_9$ by the HR-ESI-MS ion peak at *m/z* 433.1472 [M + Na]$^+$ (calcd for C$_{20}$H$_{26}$O$_9$Na, 433.1469) and 1D NMR spectral data analysis, which was two mass units more than that of **8**. The ^{1}H and ^{13}C NMR spectra of **9** exhibited similar signals to those of **8** (Tables S1 and S3), except for the signal assigned to a ketone carbonyl (δ_C 197.0, C-2 in **8**) was replaced by the signals of an oxygenated methine [δ_H 4.55 (1H, overlapped); δ_C 72.5] in **9**. Thus, compound **9** was assumed to be a C-2 hydroxylated derivative of **8**. This deduction was further verified by the spin system from H-1 to H-3 in the ^{1}H–^{1}H COSY spectrum of **9** (Figure 2). Furthermore, the α-orientation of the 2-OH was determined on the basis of key NOE correlation between H-2 and H$_3$-19 (Figure 3). A further crystallographic analysis led to the unambiguous establishment of the structure and absolute configuration (1*S*,2*S*,5*S*,7*R*,8*R*,9*R*,10*S*,11*S*,13*R*,14*R*,15*R*) of **9** (Figure 4).

The molecular formula of **10** was deduced to be identical to that of **9** on the basis of its HR-ESI-MS data (*m/z* 433.1470 [M + Na]$^+$; calcd for C$_{20}$H$_{26}$O$_9$Na, 433.1469) and ^{13}C NMR data. Comparison of the NMR data of **10** with those of **9** (Tables S1 and S3) indicated that **10** possessed the identical gross structure to **9**. The main differences of the NMR spectral data between **10** and **9** were the obvious down-field shifts of C-5 ($\Delta\delta$ +5.1) and C-6 ($\Delta\delta$ +5.2) in **10**, suggesting that **10** might be a C-5 epimer of **9**. Further analysis of its 2D NMR spectroscopic data verified that **10** possessed the identical planar structure to **9**. In the NOESY spectrum, NOE correlation between H-5 and H$_3$-19 was observed, suggesting the β-orientation for H-5 in **10** (Figure 3). Similar to **1**–**9**, the single-crystal X-ray diffraction study (Cu Kα) allowed the assignment of the complete stereochemistry of **10**. As a result, the absolute configuration of **10** was definitively assigned to be 1*S*,2*S*,5*R*,7*R*,8*R*,9*R*,10*S*,11*S*,13*R*,14*R*,15*R* (Figure 4).

2.3. Anti-proliferation Activities of Isolated Quassinoids

The isolated compounds were tested for their anti-proliferation activities on two human leukemia cell lines, K562 and HL-60. As shown in Table S5, compounds **5**, **12**, **13**, and **14** exhibited potent inhibitory effects on the proliferation of both K562 and HL-60 cells with IC$_{50}$ values ranging from 2.90 to 8.20 μM.

3. Materials and Methods

3.1. General Methods

Melting points were measured on an X-5 melting point instrument (Fukai, Beijing, China) without correction. Optical rotations were determined in MeOH on a P-1020 polarimeter (JASCO, Tokyo, Japan) with a 1 cm cell at room temperature. UV spectra

were acquired on a JASCO V-500 UV/vis spectrometer. IR spectra were obtained with a JASCO FT/IR-480 plus infrared spectrometer using KBr pellets. HR-ESI-MS data were collected using an Agilent 6210 TOF-MS spectrometer (Agilent Technologies, Santa Clara, CA, USA). Other experimental procedures were performed as described previously [14]. The human leukemia cell lines, HL-60 and K562, were purchased from the American Type Culture Collection (ATCC) and cultured in RPMI-1640 medium supplemented with 10% fetal bovine serum (FBS) and 2 mM L-glutamine.

3.2. Plant Material

The roots of *Eurycoma longifolia* were collected from Malacca, Malaysia, in June 2014 and authenticated by Prof. Guang-Xiong Zhou (College of Pharmacy, Jinan University). A voucher specimen (No. 20140501) was deposited in the Center for Bioactive Natural Molecules and Innovative Drugs Research, College of Pharmacy, Jinan University.

3.3. Extraction and Isolation

The air-dried and powdered roots of *E. longifolia* (10 kg) were extracted with 95% (*v/v*) EtOH five times at room temperature. The combined EtOH extract was concentrated under vacuum to yield a crude extract (270 g), which was suspended in water and then partitioned successively with petroleum ether, ethyl acetate, and *n*-BuOH.

The ethyl acetate-soluble fraction (95 g) was subjected to silica gel column chromatography using gradient mixture of $CHCl_3$-MeOH (100:0 → 0:100, *v/v*) as eluent to afford 10 major fractions (Fr.1–Fr.10).

Fr.2 (30.5 g) was further separated on a silica gel column (petroleum ether-EtOAc, 100:0 → 0:100, *v/v*) to give six subfractions Fr.2A–Fr.2F. Fr.2B (1.2 g) was purified by a Sephadex LH-20 column ($CHCl_3$-MeOH, 1:1) followed by semipreparative HPLC (CH_3CN-H_2O, 35:65, *v/v*) to yield compounds **2** (5.0 mg) and **4** (8.0 mg). Then, Fr.2D (15.0 g) was separated over an ODS column (MeOH-H_2O, 20:80 → 100:0) to afford six subfractions (Fr.2D-1–Fr.2D-6). Fr.2D-2 (3.0 g) was subsequently purified by semipreparative HPLC (MeOH-H_2O, 30:70, *v/v*) to give compounds **1** (14.5 mg) and **11** (8.4 mg), and Fr.2D-4 (1.5 g) was also purified by preparative HPLC (MeOH-H_2O, 35:65, *v/v*) to afford compound **3** (6.0 mg). Fr.3 (5.0 g) was applied to a Sephadex LH-20 column (MeOH) and gave five subfractions Fr.3A–Fr.3E. Furthermore, Fr.3B was further subjected to preparative HPLC (MeOH-H_2O, 32:68, *v/v*) to give compound **12** (45.0 mg).

Fr. 6 (20.0 g) was purified over an ODS column using MeOH-H_2O (20:80 → 100:0, *v/v*) as eluent to afford eight subfractions (Fr.6A–Fr.6H). Fr.6B (8.0 g) was subjected to a Sephadex LH-20 column (MeOH) to yield five subfractions (Fr.6B-1–Fr.6B-5). Fr.6B-2 (3.0 g) was purified by semipreparative HPLC (CH_3CN-H_2O, 18:82, *v/v*) to give compounds **5** (7.4 mg), **6** (10.0 mg), **7** (40.5 mg), and **13** (1.5 g), respectively. Fr.6B-4 (500 mg) was purified by preparative HPLC (CH_3CN-H_2O, 18:82, *v/v*) to give compounds **8** (25.3 mg), **9** (5.2 mg), and **10** (5.1 mg).

Fr.9 (3.5 g) was applied to a Sephadex LH-20 column (MeOH) to obtain four subfractions Fr.9A–Fr.9D. Then, Fr.9C (1.2 g) was further subjected to preparative HPLC separation (CH_3CN-H_2O, 12:88, *v/v*) to afford compound **14** (80 mg).

3.4. Compounds Characterization

Longifolactone G (**1**): colorless needles (MeOH); mp 290–291 °C; $[\alpha]_D^{25}$ +58.0 (*c* 0.55, MeOH); UV (CH_3CN) λ_{max} (log *ε*): 241 (3.81) nm; IR (KBr) ν_{max} 3455, 2957, 1730, 1667, 1432, 1379, 1348, 1229, 1198, 1115, 1017, 973, 878 cm^{-1}; ^{1}H and ^{13}C NMR spectral data, see Tables S1 and S2; HR-ESI-MS *m/z* 395.1696 [M + H]$^+$ (calcd for $C_{20}H_{27}O_8$, 395.1700).

Longifolactone H (**2**): colorless needles (MeOH); mp 225–226 °C; $[\alpha]_D^{25}$ −6.2 (*c* 0.34, MeOH); UV (CH_3CN) λ_{max} (log *ε*): 241 (4.01) nm; IR (KBr) ν_{max} 3432, 2941, 1725, 1662, 1380, 1262, 1122, 998, 819, 564 cm^{-1}; ^{1}H and ^{13}C NMR spectral data, see Tables S1 and S2; HR-ESI-MS *m/z* 433.1832 [M + Na]$^+$ (calcd for $C_{21}H_{30}O_8Na$, 433.1833).

Longifolactone I (**3**): colorless needles (MeOH); mp 178–179 °C; $[\alpha]_D^{25}$ +56.0 (*c* 0.46, MeOH); UV (CH$_3$CN) λ_{max} (log ε); 230 (3.97) nm; IR (KBr) v_{max}: 3468, 3346, 2953, 2904, 2577, 1727, 1496, 1411, 1316, 1226, 1128, 1057, 1015, 963, 813, 712, 638 cm^{-1}; ^{1}H and ^{13}C NMR spectral data, see Tables S1 and S2; HR-ESI-MS: *m/z* 371.1831 [M + Na]$^+$ (calcd for C$_{20}$H$_{28}$O$_5$Na, 371.1829).

Longifolactone J (**4**): colorless needles (MeOH); mp 255–256 °C; $[\alpha]_D^{25}$ +18.2 (c 0.29, MeOH); UV (CH$_3$CN) λ_{max} (log ε): 241 (3.75) nm; IR (KBr) v_{max} 3450, 2943, 1726, 1656, 1434, 1379, 1347, 1261, 1196, 1123, 1063, 998, 959, 589, 523 cm^{-1}; ^{1}H and ^{13}C NMR spectral data, see Tables S1 and S2; HR-ESI-MS *m/z* 401.1574 [M + Na]$^+$ (calcd for C$_{20}$H$_{26}$O$_7$Na, 401.1571).

Longifolactone K (**5**): colorless needles (MeOH-C$_5$H$_5$N); mp 266–267 °C; $[\alpha]_D^{25}$ −7.2 (c 0.31, MeOH); UV (CH$_3$CN) λ_{max} (log ε): 240 (4.01) nm; IR (KBr) v$_{max}$ 3429, 2944, 1726, 1660, 1435, 1381, 1261, 1122, 1064, 997, 964, 902, 819, 698, 449 cm^{-1}; ^{1}H and ^{13}C NMR spectral data, see Tables S1 and S2; HR-ESI-MS m/z 401.1574 [M + Na]$^+$ (calcd for C$_{20}$H$_{26}$O$_7$Na, 401.1571).

Longifolactone L (**6**): colorless needles (MeOH); mp 265–266 °C, $[\alpha]_D^{25}$ +22.2 (*c* 0.92, MeOH); UV (CH$_3$CN) λ_{max} (log ε): 195 (3.80) nm; IR (KBr) v_{max}: 3468, 3354, 2951, 2904, 2719, 1729, 1499, 1389, 1314, 1226, 1125, 1055, 964, 814 cm^{-1}; ^{1}H and ^{13}C NMR spectral data, see Tables S1 and S3; HR-ESI-MS *m/z* 435.1626 [M + Na]$^+$ (calcd for C$_{20}$H$_{28}$O$_9$Na, 435.1626).

Longifolactone M (**7**): colorless needles (MeOH); mp 300–301 °C; $[\alpha]_D^{25}$ +10.1 (*c* 0.70, MeOH); UV (CH$_3$CN) λ_{max} (log ε): 198 (3.60) nm; IR (KBr) v_{max} 3304, 2886, 1737, 1654, 1507, 1456, 1426, 1332, 1281, 1234, 1081, 993, 917 cm^{-1}; ^{1}H and ^{13}C NMR spectral data, see Tables S1 and S3; HR-ESI-MS *m/z* 435.1621 [M + Na]$^+$ (calcd for C$_{20}$H$_{28}$O$_9$Na, 435.1626).

Longifolactone N (**8**): colorless needles (MeOH); mp 248–249 °C, $[\alpha]_D^{25}$ +44.6 (*c* 0.67, MeOH); UV (CH$_3$CN) λ_{max} (log ε): 240 (3.46) nm; IR (KBr) v_{max}: 3495, 3324, 1739, 1664, 1491, 1394, 1252, 1155, 1108, 1066, 973, 823 cm^{-1}; ^{1}H and ^{13}C NMR spectral data, see Tables S1 and S3; HR-ESI-MS *m/z* 431.1311 [M + Na]$^+$ (calcd for C$_{20}$H$_{24}$O$_9$Na, 431.1313).

Longifolactone O (**9**): colorless needles (MeOH); mp 245–246 °C, $[\alpha]_D^{25}$ +4.2 (*c* 3.07, MeOH); UV (CH$_3$CN) λ_{max} (log ε): 198 (3.63) nm; IR (KBr) v_{max}: 3307, 2915, 1737, 1659, 1489, 1434, 1389, 1192, 1156, 1104, 974 cm^{-1}; ^{1}H and ^{13}C NMR spectral data, see Tables S1 and S3; HR-ESI-MS: *m/z* 433.1472 [M + Na]$^+$ (calcd for C$_{20}$H$_{26}$O$_9$Na, 433.1469).

Longifolactone P (**10**): colorless needles (MeOH); mp 265–266 °C; $[\alpha]_D^{25}$ −1.3 (*c* 0.15, MeOH); UV (CH$_3$CN) λ_{max} (log ε): 196 (3.70) nm; IR (KBr) v_{max}: 3491, 3305, 1739, 1661, 1389, 1250, 1154, 1108, 1064, 975, 835 cm^{-1}; ^{1}H and ^{13}C NMR spectral data, see Tables S1 and S3; HR-ESI-MS *m/z* 433.1470 [M + Na]$^+$ (calcd for C$_{20}$H$_{26}$O$_9$Na, 433.1469).

Chaparrolide (**11**): colorless needles (MeOH); mp 184–185 °C; $[\alpha]_D^{25}$ +15.6 (*c* 0.11, MeOH); UV (CH$_3$CN) λ_{max} (log ε): 196 (3.94) nm; IR (KBr) v_{max} 3484, 3369, 2961, 1720, 1381, 1242, 1098, 1054, 982, 810 cm^{-1}; ^{1}H and ^{13}C NMR spectral data, see Table S4 in Supplementary Materials; HR-ESI-MS *m/z* 389.1940 [M + Na]$^+$ (calcd for C$_{20}$H$_{30}$O$_6$Na, 389.1935).

15β-Hydroxyklaineanone (**12**): colorless needles (MeOH); mp 223–224 °C; $[\alpha]_D^{25}$ +6.3 (c 1.73, MeOH); UV (CH$_3$CN) λ_{max} (log ε): 242 (4.05) nm; IR (KBr) v_{max} 3460, 2950, 1733, 1671, 1436, 1378, 1259, 1124, 1068, 1000, 958, 902, 814, 697, 633 cm^{-1}; ^{1}H and ^{13}C NMR spectral data, see Table S4 in Supplementary Materials; HR-ESI-MS *m/z* 403.1734 [M + Na]$^+$ (calcd for C$_{20}$H$_{28}$O$_7$Na, 403.1727).

14,15β-Dihydroxyklaineanone (**13**): colorless needles (MeOH); mp 266–267 °C; $[\alpha]_D^{25}$ +54.3 (*c* 0.51, MeOH); UV (CH$_3$CN) λ_{max} (log ε): 241 (4.05) nm; IR (KBr) v_{max} 3425, 2945, 1726, 1660, 1435, 1381, 1344, 1262, 1122, 1064, 998, 964, 902, 818, 698 cm^{-1}; ^{1}H and ^{13}C NMR spectral data, see Table S4 in Supplementary Materials; HR-ESI-MS *m/z* 419.1674 [M + Na]$^+$ (calcd for C$_{20}$H$_{28}$O$_8$Na, 419.1676).

Eurycomanone (**14**): colorless needles (MeOH); mp 285–286 °C; $[\alpha]_D^{25}$ +39.5 (*c* 0.65, MeOH); UV (CH$_3$CN) λ_{max} (log ε): 241 (3.46) nm; IR (KBr) v_{max} 3402, 2981, 2880, 1736, 1676, 1622, 1504, 1435, 1312, 1231, 1121, 1056, 985, 826, 765 cm^{-1}; ^{1}H and ^{13}C NMR spectral data, see Table S4 in Supplementary Materials; HR-ESI-MS *m/z* 431.1314 [M + Na]$^+$ (calcd for C$_{20}$H$_{24}$O$_9$Na, 431.1313).

3.5. X-ray Crystallographic Analyses

The crystal data of compounds **1-10** were collected using an Oxford-Diffraction SuperNova diffractometer (Agilent Technologies, Yarnton, UK) with Cu Kα radiation. The crystal structures were solved by direct methods using the SHELXS program (Sheldrick, 2019) [23], and refined by the SHELXL-2018 program (Sheldrick, 2019) [23] and full-matrix least-squares calculation. Crystal data of compounds **1-10** in standard CIF format were deposited with the Cambridge Crystallographic Data Centre (CCDC 2,105,724 for **1**, CCDC 2,105,722 for **2**, CCDC 2,105,723 for **3**, CCDC 2,105,731 for **4**, and CCDC 2,105,730 for **5**, CCDC 2,105,729 for **6**, CCDC 2,105,727 for **7**, and CCDC 2,105,725 for **8**, CCDC 2,105,726 for **9**, and CCDC 2,105,728 for **10**).

Crystal data for compound **1** (M = 394.41 g/mol): orthorhombic, space group $P2_12_12_1$, a = 7.17350(10) Å, b = 10.18810(10) Å, c = 24.5189(2) Å, β = 90°, V = 1791.95(3) Å^3, Z = 4, T = 99.99(10) K, μ (Cu Kα) = 0.948 mm^{-1}, D_{calc} = 1.462 g/cm^3, 21,948 reflections measured ($7.21° \leq 2\theta \leq 147.054°$), 3593 unique ($R_{int}$ = 0.0301, R_{sigma} = 0.0140) which were used in all calculations. The final R_1 was 0.0306 (I > 2σ (I)), and wR_2 was 0.0807 (all data). Flack parameter = 0.06(4).

Crystal data for compound **2** (M = 410.45 g/mol): monoclinic, space group $P2_1$, a = 8.0642(2) Å, b = 10.6239(3) Å, c = 11.9568(3) Å, β = 107.411(2)°, V = 977.44(5) Å^3, Z = 2, T = 100.00(10) K, μ (Cu Kα) = 0.888 mm^{-1}, D_{calc} = 1.395 g/cm^3, 9576 reflections measured ($7.75° \leq 2\theta \leq 146.844°$), 3595 unique ($R_{int}$ = 0.0302, R_{sigma} = 0.0220) which were used in all calculations. The final R_1 was 0.0353 (I > 2σ (I)), and wR_2 was 0.0946 (all data). Flack parameter = 0.09(8).

Crystal data for compound **3** (M = 364.44 g/mol): monoclinic, space group $P2_1$, a = 7.0067(2) Å, b = 13.4001(4) Å, c = 9.7581(3) Å, β = 90.421(2)°, V = 916.17(5) Å^3, Z = 2, T = 293(2) K, μ (Cu Kα) = 0.795 mm^{-1}, D_{calc} = 1.328 g/cm^3, 8696 reflections measured ($9.062° \leq 2\theta \leq 147.176°$), 3440 unique ($R_{int}$ = 0.0639, R_{sigma} = 0.0435) which were used in all calculations. The final R_1 was 0.0355 (I > 2σ (I)), and wR_2 was 0.0908 (all data). Flack parameter = 0.09(9).

Crystal data for compound **4** (M = 378.41 g/mol): orthorhombic, space group $P2_12_12_1$, a = 9.63490(10) Å, b = 12.0407(2) Å, c = 15.6703(2) Å, β = 90°, V = 1817.93(4) Å^3, Z = 4, T = 100.00(10) K, μ (Cu Kα) = 0.868 mm^{-1}, D_{calc} = 1.383 g/cm^3, 14,343 reflections measured ($9.262° \leq 2\theta \leq 146.826°$), 3607 unique ($R_{int}$ = 0.0285, R_{sigma} = 0.0201) which were used in all calculations. The final R_1 was 0.0284 (I > 2σ (I)), and wR_2 was 0.0746 (all data). Flack parameter = −0.05(6).

Crystal data for compound **5** (M = 457.51 g/mol): monoclinic, space group I2, a = 7.84600(10) Å, b = 12.85380(10) Å, c = 22.0124(2) Å, β = 95.8390(10)°, V = 2208.45(4) Å^3, Z = 4, T = 100.00(10) K, μ (Cu Kα) = 0.828 mm^{-1}, D_{calc} = 1.376 g/cm^3, 20,973 reflections measured ($7.976° \leq 2\theta \leq 147.044°$), 4407 unique ($R_{int}$ = 0.0497, R_{sigma} = 0.0283) which were used in all calculations. The final R_1 was 0.0334 (I > 2σ (I)), and wR_2 was 0.0884 (all data). Flack parameter = 0.05(7).

Crystal data for compound **6** (M = 466.47 g/mol): orthorhombic, space group $P2_12_12_1$, a = 13.8037(6) Å, b = 12.1850(6) Å, c = 12.0498(5) Å, β = 90°, V = 2026.75(16) Å^3, Z = 4, T = 113(20) K, μ (Cu Kα) = 1.079 mm^{-1}, D_{calc} = 1.529 g/cm^3, 7421 reflections measured ($7.336° \leq 2\theta \leq 147.508°$), 3904 unique ($R_{int}$ = 0.0401, R_{sigma} = 0.0517) which were used in all calculations. The final R_1 was 0.0503 (I > 2σ (I)), and wR_2 was 0.1464 (all data). Flack parameter = −0.04(9).

Crystal data for compound **7** (M = 430.44 g/mol): orthorhombic, space group $P2_12_12_1$, a = 6.94750(10) Å, b = 9.86740(10) Å, c = 28.8229(4) Å, β = 90°, V = 1975.92(4) Å^3, Z = 4, T = 100.00(10) K, μ (Cu Kα) = 0.983 mm^{-1}, D_{calc} = 1.447 g/cm^3, 22,539 reflections measured ($6.132° \leq 2\theta \leq 147.044°$), 3946 unique ($R_{int}$ = 0.0695, R_{sigma} = 0.0368) which were used in all calculations. The final R_1 was 0.0372 (I > 2σ (I)), and wR_2 was 0.1016 (all data). Flack parameter = −0.12(9).

Crystal data for compound **8** (M = 480.45 g/mol): orthorhombic, space group $P2_12_12_1$, a = 7.02070(10) Å, b = 13.3311(2) Å, c = 22.4885(3) Å, β = 90°, V = 2104.78(5) Å^3, Z = 4,

T = 100.01(10) K, μ (Cu Kα) = 1.097 mm^{-1}, D$_{calc}$ = 1.516 g/cm^3, 20,217 reflections measured (7.71° ≤ 2θ ≤ 147.848°), 4187 unique (R$_{int}$ = 0.0429, R$_{sigma}$ = 0.0296) which were used in all calculations. The final R$_1$ was 0.0282 (I > 2σ (I)), and wR$_2$ was 0.0734 (all data). Flack parameter = −0.01(6).

Crystal data for compound **9** (M = 410.41 g/mol): monoclinic, space group C2, a = 17.7027(6) Å, b = 8.4150(3) Å, c = 12.3274(3) Å, β = 99.070(3)°, V = 1813.43(10) Å^3, Z = 4, T = 100.00(10) K, μ (Cu Kα) = 1.004 mm^{-1}, D$_{calc}$ = 1.503 g/cm^3, 16,975 reflections measured (7.262° ≤ 2θ ≤ 147.362°), 3635 unique (R$_{int}$ = 0.0514, R$_{sigma}$ = 0.0313) which were used in all calculations. The final R$_1$ was 0.0388 (I > 2σ (I)), and wR$_2$ was 0.1080 (all data). Flack parameter = 0.10(9).

Crystal data for compound **10** (M = 428.42 g/mol): orthorhombic, space group P2$_1$2$_1$2$_1$, a = 7.2511(2) Å, b = 10.6856(3) Å, c = 24.0611(9) Å, β = 90°, V = 1864.31(10) Å^3, Z = 4, T = 100.00(10) K, μ (Cu Kα) = 1.042 mm^{-1}, D$_{calc}$ = 1.526 g/cm^3, 17,396 reflections measured (7.348° ≤ 2θ ≤ 147.984°), 3693 unique (R$_{int}$ = 0.0511, R$_{sigma}$ = 0.0405) which were used in all calculations. The final R$_1$ was 0.0375 (I > 2σ (I)), and wR$_2$ was 0.0896 (all data). Flack parameter = 0.07(10).

3.6. Cell Proliferation Assay

HL-60 and K562 cells were cultured in 96-well plates and incubated at 37 °C, 5% CO$_2$ incubator. After incubation for 24 h, the cell supernatants were discarded and supplemented with cell culture medium containing compounds at different concentrations. At 48 h after incubation, the cell supernatants in each well were removed and replaced with 100 μL culture medium containing 10 μL of cell counting kit-8 (Sigma-Aldrich, St. Louis, MO, USA), followed by incubation at 37 °C, 5% CO$_2$ for 2 h. The absorbance at 450 nm of the cells was measured using a Plate Reader. Cell proliferation was calculated according to the OD$_{450}$ value in cells that were treated with or without compounds.

4. Conclusions

In summary, a further phytochemical study on the roots of the medicinal plant *Eurycoma longifolia* resulted in the isolation and characterization of 14 highly oxygenated C$_{20}$ quassinoids, including 10 new ones (longifolactones G-P, **1**–**10**). Structurally, compound **1** is the second member of a rare class of quassinoids featuring an unusual 2,5-dioxatricyclo[5.2.2.0^{4,8}]undecane ring system. Compound **4** possesses a 14,15-epoxy functionality that is unprecedented in quassinoids, and compound **7** features an unusual α-oriented hydroxyl group at C-14. In addition, compounds **5**, **12**, **13**, and **14** showed potent anti-proliferation activities on two human leukemia cell lines, K562 and HL-60.

Author Contributions: W.-Q.Y. and W.T. performed the isolation, purification, structure determination, and written the manuscript. X.-J.H. performed the structural identification of the compounds. J.-G.S. conducted the single crystal X-ray diffraction experiments. Y.-Y.L. worked in biological experiments. Y.X. and C.-L.F. performed the extraction, isolation and structural identification of the compounds. Y.W., Z.-L.W., and W.-C.Y. designed the whole experiments and revised the paper. All authors have read and agreed to the published version of the manuscript.

Institutional Review Board Statement: Not applicable.

Informed Consent Statement: Not applicable.

Data Availability Statement: All data supporting this study is available in the manuscript and the Supplementary Materials.

Conflicts of Interest: The authors declare no conflict of interest.

Sample Availability: Samples of the compounds **1**–**14** are available from the authors.

References

1. Guo, Z.; Vangapandu, S.; Sindelar, R.W.; Walker, L.A.; Sindelar, R.D. Biologically active quassinoids and their chemistry: Potential leads for drug design. *Curr. Med. Chem.* **2005**, *12*, 173–190. [CrossRef] [PubMed]
2. Duan, Z.K.; Zhang, Z.J.; Dong, S.H.; Wang, Y.X.; Song, S.J.; Huang, X.X. Quassinoids: Phytochemistry and antitumor prospect. *Phytochemistry* **2021**, *187*, 112769. [CrossRef] [PubMed]
3. Zhao, W.Y.; Song, X.Y.; Zhao, L.; Zou, C.X.; Zhou, W.Y.; Lin, B.; Yao, G.D.; Huang, X.X.; Song, S.J. Quassinoids from *Picrasma quassioides* and their neuroprotective effects. *J. Nat. Prod.* **2019**, *82*, 714–723. [CrossRef]
4. Polonsky, J. Quassinoid bitter principles. *Fortschr. Chem. Org. Naturst.* **1973**, *30*, 101–150. [PubMed]
5. Polonsky, J. Quassinoid bitter principles II. *Prog. Chem. Org. Nat. Prod.* **1985**, *47*, 221–264. [CrossRef]
6. Ravindar, K.; Caron, P.Y.; Deslongchamps, P. Anionic polycyclization entry to tricycles related to quassinoids and terpenoids: A stereocontrolled total synthesis of (+)-cassaine. *J. Org. Chem.* **2014**, *79*, 7979–7999. [CrossRef]
7. Condakes, M.L.; Rosen, R.Z.; Harwood, S.J.; Maimone, T.J. A copper-catalyzed double coupling enables a 3-step synthesis of the quassinoid core architecture. *Chem. Sci.* **2019**, *10*, 768–772. [CrossRef]
8. Bhat, R.; Karim, A.A. Tongkat Ali (*Eurycoma longifolia* Jack): A review on its ethnobotany and pharmacological importance. *Fitoterapia* **2010**, *81*, 669–679. [CrossRef] [PubMed]
9. Nurhanan, M.Y.; Hawariah, L.P.A.; Ilham, A.M.I.; Shukri, M.A.M. Cytotoxic effects of the roots extracts of *Eurycoma longifolia*. *Phytother. Res.* **2005**, *19*, 994–996. [CrossRef]
10. Rehman, S.U.; Choe, K.; Yoo, H.H. Review on a traditional herbal medicine, *Eurycoma longifolia* Jack (Tongkat Ali): Its traditional uses, chemistry, evidence-based pharmacology and toxicology. *Molecules* **2016**, *21*, 331. [CrossRef]
11. Wong, P.F.; Cheong, W.F.; Shu, M.H.; The, C.H.; Chan, K.L.; AbuBakar, S. Eurycomanone suppresses expression of lung cancer tumor markers, prohibitin, annexin 1 and endoplasmic reticulum protein 28. *Phytomedicine* **2012**, *19*, 138–144. [CrossRef] [PubMed]
12. Tung, N.H.; Uto, T.; Hai, N.T.; Li, G.; Shoyama, Y. Quassinoids from the roots of *Eurycoma longifolia* and their antiproliferative activity on human cancer cell lines. *Pharmacogn. Mag.* **2017**, *13*, 459–462.
13. Hajjouli, S.; Chateauvieux, S.; Teiten, M.H.; Orlikova, B.; Schumacher, M.; Dicato, M.; Choo, C.Y.; Diederich, M. Eurycomanone and eurycomanol from *Eurycoma longifolia* Jack as regulators of signaling pathways involved in proliferation, cell death and inflammation. *Molecules* **2014**, *19*, 14649–14666. [CrossRef] [PubMed]
14. Yang, W.Q.; Shao, X.H.; Deng, F.; Hu, L.J.; Xiong, Y.; Huang, X.J.; Fan, C.L.; Jiang, R.W.; Ye, W.C.; Wang, Y. Unprecedented quassinoids from *Eurycoma longifolia*: Biogenetic evidence and antifeedant effects. *J. Nat. Prod.* **2020**, *83*, 1674–1683. [CrossRef]
15. Mitchell, R.E.; Stocklin, W.; Stefanovic, M.; Geissman, T.A. Chaparrolide and castelanolide, new bitter principles from *Castela nicholsoni*. *Phytochemistry* **1971**, *10*, 411–417. [CrossRef]
16. Polonsky, J.; Baskevitch, Z.; Gottlieb, H.E.; Hagaman, E.W.; Wenkert, E. Carbon-13 nuclear magnetic resonance spectral analysis of quassinoid bitter principles. *J. Org. Chem.* **1975**, *40*, 2499–2504. [CrossRef]
17. Chan, K.L.; Lee, S.P.; Sam, T.W.; Tan, S.C.; Noguchi, H.; Sankawa, U. 13β,18-dihydroeurycomanol, a quassinoid from *Eurycoma longifolia*. *Phytochemistry* **1991**, *30*, 3138–3141. [CrossRef]
18. Morita, H.; Kishi, E.; Takeya, K.; Itokawa, H.; Tanaka, O. New quassinoids from the roots of *Eurycoma longifolia*. *Chem. Lett.* **1990**, *19*, 749–752. [CrossRef]
19. Morita, H.; Kishi, E.; Takeya, K.; Itokawa, H.; Iitaka, Y. Highly oxygenated quassinoids from *Eurycoma longifolia*. *Phytochemistry* **1993**, *33*, 691–696. [CrossRef]
20. Itokawa, H.; Kishi, E.; Morita, H.; Takeya, K. Cytotoxic quassinoids and tirucallane-type triterpenes from the woods of *Eurycoma longifolia*. *Chem. Pharm. Bull.* **1992**, *40*, 1053–1055. [CrossRef]
21. Meng, D.L.; Li, X.; Han, L.F.; Zhang, L.L.; An, W.W.; Li, X. Four new quassinoids from the roots of *Eurycoma longifolia*. *Fitoterapia* **2014**, *82*, 105–110. [CrossRef] [PubMed]
22. Miyake, K.; Tezuka, Y.; Awale, S.; Li, F.; Kadota, S. Quassinoids from *Eurycoma longifolia*. *J. Nat. Prod.* **2009**, *72*, 2135–2140. [CrossRef] [PubMed]
23. Lübben, J.; Wandtke, C.M.; Hübschle, C.B.; Ruf, M.; Sheldrich, G.M.; Dittrich, B. Aspherical scattering factors for SHELXL-model, implementation and application. *Acta Crystallogr. A* **2019**, *75*, 50–62. [CrossRef] [PubMed]